ÉCOLE POLYTECHNIQUE
FÉDÉRALE DE LAUSANNE

2004.6

LESO-PB

Designing thin film multilayers for colored glazed thermal collectors

Schueler A., Roecker C., Scartezzini J.-L. (EPFL)
Boudaden J., Oelhafen P. (Universität Basel)

Proceedings of EUROSUN 2004, Freiburg in Brisgau (D)

June 2004

Designing thin film multilayers for colored glazed thermal collectors

A. Schüler, C. Roecker, J.-L. Scartezzini
Laboratoire d'Energie Solaire et de Physique du Bâtiment LESO-PB, Ecole Polytechnique Fédérale de Lausanne EPFL, Bâtiment LE, 1015 Lausanne, Switzerland
J. Boudaden, P. Oelhafen
Institut für Physik der Universität Basel, Klingelbergstr. 82, 4056 Basel, Switzerland

Multilayered interference filters of dielectric thin films have been designed for the application as energy-efficient coloration of collector cover glasses. The optical behavior of the designed multilayers is analysed by computer simulations yielding the CIE color coordinates, the relative luminosity, the degree of solar transmission, and a figure of merit which is a measure for the energy effectiveness of the coloration. A high performance should be achieved with a number of individual layers reasonable for large scale deposition. Constraints on the refractive index of the dielectric films are given by the availability of suitable thin film materials. The challenge lies in finding the best combination of material choice and layer thicknesses. We describe several types of multilayer designs for which the computer simulations yield promising results.

Motivation

06

The issue of color becomes more and more important for thermal solar collectors, and has attracted interest recently [1-3]. This might be related to a generally growing attention towards architectural integration of solar energy systems into buildings [4-7]. A recent opinion poll [1] showed, that 85% of architects would prefer different colors besides black, even if a lower efficiency would have to be accepted. Thermal solar collectors, typically equipped with black, optical selective absorber sheets, exhibit in general good energy conversion efficiencies. However, the black color, and sometimes the visibility of tubes and corrugations of the metal sheets, limits the architectural integration into buildings.
One solution to this problem is to color the absorber sheets. Optical selective absorber coatings are usually deposited by processes such as magnetron sputtering [8-10], vacuum evaporation [11], electrochemical processes [12], sol-gel technology [13], or as selective paint (thickness-sensitive or thickness-insensitive) [3,14]. Niklasson and Granqvist described the pioneering work in this area within a comprehensive overview [15]. Modifying the parameters of the deposition process can result in a colored appearance. Following this approach, the absorber surface combines the functions of optical selectivity (high solar absorption/low thermal emission) and colored reflection. Tripanagnostopoulos reports a different solution: his group used non-selective colorful paints as absorber coatings for glazed and unglazed collectors, and compensated the energy losses by additional booster reflectors [16]. Alternatively, we propose to establish a colored reflection not from the absorber but from the cover glass. This approach has the advantage that the black, sometimes ugly absorber sheet is then hidden by the colored reflection. In addition to that, the functions of optical selectivity and colored reflection are separated, giving more freedom to layer optimization. No energy should be lost by absorption in the coating: all energy, which is not reflected, should be transmitted. Therefore, multilayer interference stacks of transparent materials should be ideally suited for this purpose. A recent feasibility study showed encouraging results [17]. By employing optical methods such as real-time laser reflectometry, spectroscopic ellipsometry and spectrophotometry, the deposition of multilayered interference stacks can be monitored very precisely [18]. In this article we

describe a variety of multilayer designs, which can be employed to achieve the desired characteristics.

Theory

The propagation of electromagnetic waves in stratified media has been discussed by Born and Wolf [19]. The field of optics of thin films has been reviewed by various authors, e.g. Heavens [20], Holland [21], Anders [22], Knittl [23], and Macleod [24]. Due to the multiple reflections between the different interfaces, the problem of the optical behaviour of a multilayered thin film stack is non-trivial. It can be treated, though, by the method of characteristic matrices, which defines one matrix M_r per individual layer. From this matrix product, transmission and reflectance spectra can be computed. Extended calculations are usually carried out by a computer.

The visible reflectance R_{VIS} is a measure for the brightness of a surface as it appears to the human eye under certain illumination conditions. Its determination is based on the photopic luminous efficiency function $V(\lambda)$ and depends on the choice of the illuminant $I_{ILL}(\lambda)$:

$$R_{VIS} = \frac{\int R(\lambda) \cdot I_{ILL}(\lambda) \cdot V(\lambda) d\lambda}{\int I_{ILL}(\lambda) \cdot V(\lambda) d\lambda} \quad , \tag{1}$$

where $R(\lambda)$ is the simulated or measured hemispherical reflectance of the sample.

For the assessment of colored solar collectors it is useful to introduce a figure of merit. In a previous publication [17] we defined the ratio of the visible reflectance R_{VIS} under daylight illumination D_{65} and the solar reflectance R_{sol} (based on the solar spectrum AM1.5 global[25,26]) as figure of merit M:

$$M = (R_{VIS} \text{ under daylight illumination } D_{65}) \ / \ (R_{sol} \text{ for AM1.5 global}) \tag{2}$$

Being large in the case of high visible reflectance or low solar energy losses R_{sol}, this number describes the energy efficiency of the visual perception ("brightness per energy cost").

An alternative approach is to use for both the evaluation of the visual impression and the energetic reflection losses the same illuminant I_{sol}.

$$M' = (R_{VIS} \text{ under solar illumination AM1.5 global}) \ / \ (R_{sol} \text{ for AM1.5 global}) \tag{3}$$

In practice, the resulting values for M and M' are always rather close to each other. It can be shown that the principal upper limit for M and M' amounts to the value of approx. six (in the ideal case). Of course the energy-effectiveness of the colored reflection should not be the only criterion for the evaluation of a colored collector glazing. A sufficient solar transmission is certainly one of the most important requirements.

Simulations

a) Two-layered systems

From the field of anti-reflection coatings, two-layered coating designs such as the V- and the W-design are known [24]. These systems owe their name to the shape of the reflection minimum. The effect of anti-reflection extends over a certain wavelength range, but aside from this region considerable reflectance peaks occur, which can be used to produce a colored reflection. The region of antireflection enhances the solar transmission. Creating a region of higher reflectance at short wavelengths, blue and green colors of reflection can be easily achieved in combination with a good solar transmission. As an example we show the W-design. Both sides of the substrate are coated identically, as it occurs often in sol-gel dip coating. Our calculation takes into account the multiple reflections between the two sides. The optical model has the structure

air // L 2H // glass /2HL // air,

where the letters "L" and "H" mean quarterwave layers of low and high refractive index, respectively. The corresponding layer thicknesses t(L) and t(H) have thus been chosen to $n \times t(H) = \lambda_0/2$ and $n \times t(L) = \lambda_0/4$, where the so-called "design wavelength λ_0" indicates the center of the region of anti-reflection (here: λ_0 = 800 nm). A refractive index of 1.52 has been assumed for the glass substrate. The resulting reflectance spectra are displayed in Fig.1. For the shown examples, the resulting colors are in the region of bluish green. Within a rather large region the reflectance is lower than the one of an uncoated substrate (approx. 8%). Due to the partial antireflection, the achieved color saturation and as well the solar transmission are remarkable. A survey of the characteristic figures, the color coordinates x and y, the visible reflectance R_{VIS}, the solar transmission T_{sol} and the figure of merit $M = R_{VIS}/R_{sol}$, is given in TABLE I.

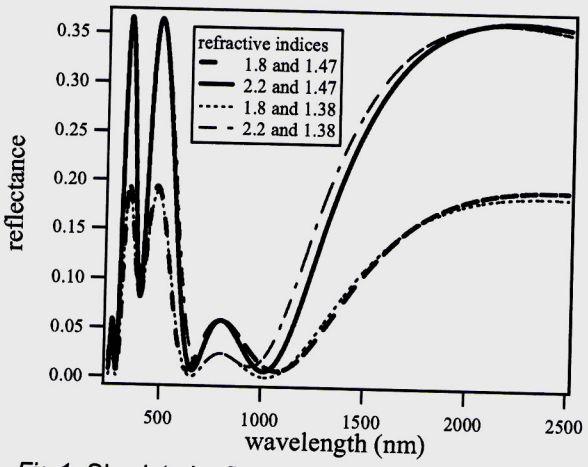

Fig.1: Simulated reflectance spectra for W-designs. The glass substrate has been assumed to be coated at both sides (optical model: air//L2H//glass//2HL//air. The design wavelength λ_0 has been chosen to 800 nm.

TABLE I:

n(H)	n(L)	t(H) [nm]	t(L) [nm]	x	y	R_{VIS} [%]	T_{sol} [%]	$M = R_{VIS}/R_{sol}$
1.8	1.47	222	136	0.18	0.27	9.1	93	1.21
2.2	1.47	182	136	0.21	0.32	21	86	1.53
1.8	1.38	222	145	0.19	0.29	9.4	93	1.42
2.2	1.38	182	145	0.23	0.34	23	86	1.63

CIE color coordinates x and y, the visible reflectance R_{VIS}, the solar transmission T_{sol} and the figure of merit $M = R_{VIS}/R_{sol}$, as computed for the curves displayed in Fig. 1.

b) Three-layered system

Starting from a classical V-design, we have studied the influence of adding a third layer. We consider a glass substrate with a refractive index of 1.52 being coated on one side by a stack of three layers, the first layer being 30 nm thick with a refractive index of 2.2, the second layer 140 nm thick with n = 1.46, and a third layer of variable thickness with n = 2.2. By variation of the thickness t3 of the topmost layer from 0 nm to 50 nm, we obtain the reflectance spectra displayed in Fig.2. The thin black line illustrates the reflectance for the two-layered V-design (thickness t3 = 0 nm). Adding the additional layer results in an increase of the colored reflection. The spectrum corresponding to the case of a 30 nm thick top layer exhibits a strong enhancement of the reflection peak and still a region of anti-reflection at a wavelength of 1000 nm. For the top layer being 50 nm thick, the region of anti-reflection is already less pronounced. Also from the point of view of the solar transmission T_{sol}(%), the region between 10 nm and 40 nm appears most interesting. TABLE II shows the numerical results for the color coordinates x and y, the visible reflectance R_{VIS}, the solar reflectance reflectance R_{sol}, the solar transmission T_{sol} and the figure of merit $M = R_{VIS}/R_{sol}$, in dependence on the thickness t3 of the third layer.

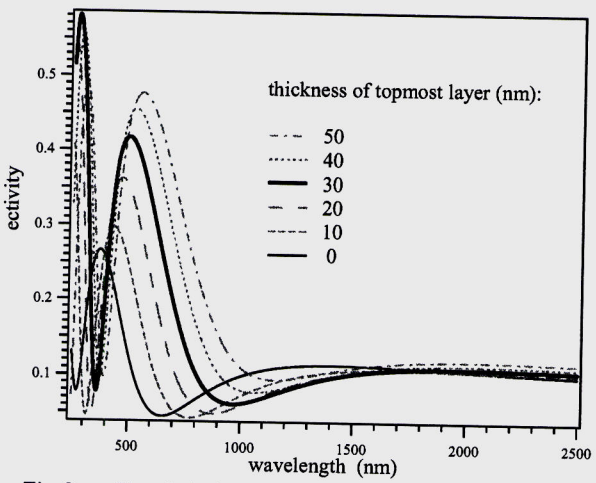

Fig.2: Simulated reflectance spectra for the three-layered system. The glass substrate has been assumed to be coated at only one side. Adding the additional layer to the V-design results in a strong enhancement of the colored reflection.

TABLE II:

t3 [nm]	x	y	R_{VIS}[%]	R_{sol}[%]	T_{sol}[%]	$M = R_{VIS}/R_{sol}$
0	0.22	0.22	8.1	10	90	0.81
10	0.24	0.27	17	12	88	1.42
20	0.27	0.31	28	16	84	1.75
30	0.29	0.34	37	20	80	1.85
40	0.31	0.36	43	24	76	1.79
50	0.34	0.38	46	27	73	1.70

CIE color coordinates x and y, the visible reflectance R_{VIS}, the solar reflectance R_{sol}, the solar transmission T_{sol} and the figure of merit $M = R_{VIS}/R_{sol}$, as computed for the curves displayed in Fig. 2.

c) Maxima of higher order

Towards shorter wavelengths, the reflectance spectra for dielectric thin film stacks exhibit rapid oscillations between the maxima and minima of higher order. By using high enough layer thicknesses, the maxima can be placed in the visible spectral region. Fig.3 illustrates an example showing the oscillations in the high wavelength region which are used for the coloration. For e.g. a color of pink two peaks, corresponding to blue and red contributions, are necessary. The calculation is based on literature data for the refractive indices of SiO_2 and TiO_2 [27-29]. For simplicity, coatings have been assumed to be transparent within the solar spectral region. Layer thicknesses of 213 nm and 258 nm are assumed for the TiO_2 and the SiO_2 layers, respectively. Color coordinates of x = 0.39 and y = 0.24 have been found, accompanied by a visible reflectance of 9.8 %, while the solar transmission amounts to 84.6 %. Some more examples are listed in TABLE III. The selection comprises two, three and four layered systems. Layer 1 is the next to the glass. A refractive index of 1.52 has been assumed for the glass, the coating is supposed to be only on one side of the substrate.

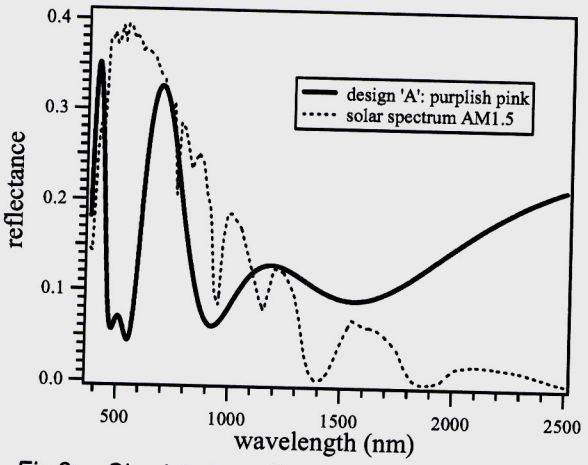

Fig.3: Simulated reflectance spectra for the design 'A' (layer 1: 213 nm TiO_2, layer 2: 258 nm SiO_2). The glass substrate has been assumed to be coated at only one side. For a color of pink two peaks, corresponding to blue and red contributions, are necessary.

06

TABLE III:

design	layer 1 TiO2 [nm]	2 SiO2 [nm]	3 TiO2 [nm]	4 SiO2 (nm)	color coordinates x	y	approx. Color	R_{VIS} [%]	T_{sol} [%]	M = R_{VIS}/R_{sol}
A	213	258			0.39	0.24	pink	9.8	85	0.64
B	126	304			0.22	0.14	blue	6.7	84	0.41
C	15	410			0.35	0.42	yellow	14	90	1.45
D	88	224			0.48	0.38	orange	16	83	0.93
E	12	378	12		0.35	0.41	yellow	17	89	1.47
F	21	45	259	109	0.22	0.15	blue	6.3	88	0.54
G	12	378	12	378	0.29	0.39	green	14	90	1.36
H	104	37	103	231	0.52	0.35	orange	16	80	0.79

Color coordinates x and y, the visible reflectance R_{VIS}, the solar reflectance R_{sol}, the solar transmission T_{sol} and the figure of merit $M = R_{VIS}/R_{sol}$, as computed for a variety of two, three and four layered systems.

d) Quarterwave stacks

In quarterwave stacks, all individual layers are of the optical film thickness $n \cdot t = \lambda_0 / 4$, where λ_0 is called the design wavelength. Usually layers of a high index material (H) alternate with layers of a low refractive index material (L), resulting in a stack of the form HLHLHL... . Often, these filters are employed as high reflectivity mirrors, exhibiting a nearly perfect reflectance over a large frequency band. The larger the difference in the refractive indices, the larger is the spectral region of high reflection. We are interested in the opposite, a narrow reflection peak, which can in principle be created by employing a large number of layers (e.g. forty layers for a linewidth in the order of 20 nm [30]). Here we consider a system, where both sides of the glass are coated each by a stack of five individual layers. Consequently, the structure of the optical model is *air//HLHLH//glass//HLHLH//air.*

The refractive indices n(H) = 1.65 and n(L) = 1.47 have been chosen (in combination with a refractive index of the glass substrate of 1.52) . Our calculation has been performed for various angles of incidence, rising from normal incidence in steps of 20°. A graphical representation is given in Fig.4, the figures are summarized in Table IV. For normal incidence, the FWHM amounts to 167 nm, the visible reflectance to 34 %. The solar transmission (84%) is acceptable; the energy loss compared to an uncoated glass amounts only to 8 % . The angular dependence of the reflectance is nicely illustrated in Fig. 4. For an angle of incidence of 20° , the curve does not change significantly; the position of the maximum shifts slightly from 550 nm to 534 nm. For 40° , the shift continues to 499 nm. For 60 °, a blueshift in the order of magnitude of the peak width is accompanied by a rise of the background level. For 80°, the background level rises further, the peak is barely distinguishable, and the properties are quite close to those of uncoated glass (representation in Fig. 4 omitted for clarity). With increasing angle of incidence, the difference between the transmission of uncoated glass T_{glass} and the transmission T_{sol} of the coated system decreases, while the figure of merit M converges to unity. In TABLE IV a survey of the characteristic numbers is given.

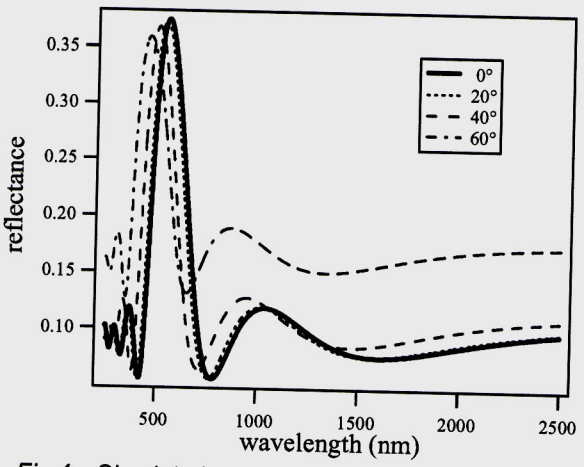

Fig.4: Simulated reflectance spectra for a design based on a five-layered quarterwave stack on each side of the glass substrate (optical model: air//HLHLH//glass//HLHLH//air. The design wavelength λ_0 has been chosen to 550 nm. Angles of reflection from 0° to 60° have been assumed.

TABLE IV:

angle	pos. max.	x	y	R_{VIS} (%)	T_{sol} (%)	T_{glass} (%)	T_{glass} - T_{sol}	M = R_{VIS}/R_{sol}
0°	548	0.35	0.44	34	84	92	8	2.1
20°	534	0.32	0.42	33	84	92	7	2.1
40°	499	0.27	0.35	29	84	91	7	1.8
60°	456	0.25	0.29	24	80	84	5	1.2
80°	-	0.30	0.33	56	45	46	1	1.0

Position of the reflectance maximum, color coordinates x and y, the visible reflectance R_{VIS}, the solar transmission T_{sol} , the transmission of an uncoated glass T_{glass}, the difference T_{glass} - T_{sol} between the latter and the solar transmission, and the figure of merit M = R_{VIS}/R_{sol}, as computed for the curves displayed in Fig. 4. The values for the angle of incidence of 80° are added.

By adapting film thicknesses according to the relation $n \cdot t = \lambda_0 / 4$, the peak position λ_0 can be shifted easily. For design wavelengths λ_0 of 450 nm and 650 nm, colors of blue (x = 0.20 , y = 0.24) and orange (x = 0.44 , y = 0.36) are attained. The solar transmission increases slightly or changes barely (6 % and 84 %, respectively), while the visible reflectance decreases (17 % and 29 %, respectively).

Discussion

06

Several design types have been proposed to achieve an energy-efficient coloration of solar collector glazing. Known anti-reflection coatings such as the two-layered V- and W-design can be modified to create a colorful reflection in the visible spectral region and a region of antireflection e.g. in the infrared. This approach is especially suitable to create blue and green colors in combination with a high solar transmission. Addition of a third layer to a V-design leads to a strong enhancement of the reflectance peak. Already with such a three-layered coating design of moderate total coating thickness, considerable peak heights and thus a strong visible reflectance can be achieved. Therefore this design is attractive for large area coating processes where production costs scale with the number of individual layers and the total coating thickness. Another way to create a colored reflection is to make use of the maxima of higher order appearing towards short wavelengths. In this regime the shapes of the reflectance spectra become rather complex, but can be used to produce colors where more than one reflection peak is needed. A systematic approach to the problem of achieving a single, isolated reflectance peak is the one of quarterwave stacks. Already with stacks of five layers and a suitable choice of refractive indices, sufficiently narrow reflectance peaks can be produced. Interference colors are in general angle-dependent. This could both increase (nice effect, high-tech image) or decrease acceptance of the proposed collector covers, which is a subject of discussion with architects, manufacturers and end-users. However, for the shown example of a five-layered quarterwave stack, the peak shift at 60° angle of reflection is in the same order of magnitude as the half peak width. Additionally, if the multilayered coating is only applied at the inner side of the collector, the angular dependence can be reduced by diffusing elements, such as rough surfaces/interfaces or a diffusing interlayer. Common thin film deposition processes are magnetron sputtering, plasma enhanced chemical vapor deposition, vacuum evaporation, or SolGel dip coating . Transparent oxides such as silicon dioxide ($n \approx 1.47$), aluminum oxide ($n \approx 1.65$) , or titanium dioxide ($n \approx 2.2$) can routinely be deposited [24,31,32]. Intermediate refractive indices would be accessible by the synthesis of mixed oxides. Nanocomposite mixed oxides can be modeled in the framework of effective medium theories, such as e.g. the Bruggeman or the Ping Sheng theory [33,34],

both providing analytical expressions for the resulting optical properties. With all coating processes, care has to be taken for a superior film homogeneity, which is essential for interference filters. Vacuum processes yield in general high quality films, but a considerable investment into the vacuum coating machines is necessary already in the start-up phase. The scale-up of a vacuum process, which has been developed in the laboratory, is possible, but non-trivial [35]. This is much easier for SolGel dip-coating. Once the right solutions and withdrawal speeds are found, the size of the glass pane does not alter the basic process parameters. Here, one main problem is to avoid dust, which creates defects and harms the coating quality. Costs rise with the repeated baking of multilayered coatings on large glass panes. One solution to the problem can be special precursors, which enable a film hardening by ultraviolet light [36].

Conclusions

Multilayered interference filters of dielectric thin films have been designed for the application as energy-efficient coloration of collector cover glasses. The optical behavior of the designed multilayers is analysed by computer simulations yielding the CIE color coordinates, the relative luminosity, the degree of solar transmission, and a figure of merit which is a measure for the energy effectiveness of the coloration. For several types of multilayer design the computer simulations yield promising results. Hereby, constraints such as a realistic choice of refractive indices, a limited number of layers in the stack, and a not excessive total stack thickness have been respected. The way for the experimental realisation of energy-efficient colored glazed solar collectors has thus been opened up.

Acknowledgements

Financial support of this work has been provided by the Swiss Federal Office of Energy SFOE. Authors are grateful to Dr. I. Hagemann, and Dr. P. W. Oliveira for inspiring discussions.

References

1. W. Weiss, I. Stadler, *Facade Integration – a new and promising opportunity for thermal solar collectors,* Proceedings of the Industry Workshop of the IEA Solar Heating and Cooling Programme, Task 26 in Delft, The Netherlands, April 2, 2001 (http://www.fys.uio.no/kjerne/task26/pdf/industry_workshop_delft.pdf)
2. I. Stadler, *Facade Integrated Solar Thermal Collectors,* Proceedings of the Congress Solar Space Heating, Graz, Austria (2001)
3. B. Orel, A. Surca Vuk, A. Vilcnik, B. Jelen, M. Köhl, M. Heck, *Thickness insensitive spectrally selective (TISS) paint coatings for glazed and unglazed solar building facades*, Proceedings of the ISES World Congress 2003, O2 45, Götheborg, Sweden
4. A. G. Hestnes, Sol. Energy **67**, Issues 4 – 6, (1999), 181
5. C. Roecker, P. Affolter, J. Bonvin, J. – B. Gay, A. N. Müller, Sol. Energy Mater. and Sol. Cells **36,** (1995), 381
6. I. B. Hagemann, *Architektonische Integration der Photovoltaik in die Gebäudehülle*, PhD thesis accepted at the Technical University of Aachen, ISBN 3-481-01776-6, Müller, Köln, 2002